Provided for non-commercial research and education use.
Not for reproduction, distribution or commercial use.

This article appeared in a journal published by Elsevier. The attached copy is furnished to the author for internal non-commercial research and education use, including for instruction at the authors institution and sharing with colleagues.

Other uses, including reproduction and distribution, or selling or licensing copies, or posting to personal, institutional or third party websites are prohibited.

In most cases authors are permitted to post their version of the article (e.g. in Word or Tex form) to their personal website or institutional repository. Authors requiring further information regarding Elsevier's archiving and manuscript policies are encouraged to visit:

http://www.elsevier.com/copyright

Author's personal copy

Journal of Colloid and Interface Science 347 (2010) 142–146

Contents lists available at ScienceDirect

Journal of Colloid and Interface Science

www.elsevier.com/locate/jcis

Wall-induced lateral migration in particle electrophoresis through a rectangular microchannel

Litao Liang [a], Ye Ai [b], Junjie Zhu [a], Shizhi Qian [b,c], Xiangchun Xuan [a,*]

[a] Department of Mechanical Engineering, Clemson University, Clemson, SC 29634-0921, USA
[b] Department of Aerospace Engineering, Old Dominion University, Norfolk, VA 23529, USA
[c] School of Mechanical Engineering, Yeungnam University, Gyongsan 712-749, South Korea

ARTICLE INFO

Article history:
Received 3 February 2010
Accepted 17 March 2010
Available online 20 March 2010

Keywords:
Particle electrophoresis
Wall effects
Lateral migration
Dielectrophoresis

ABSTRACT

The fundamental study of particle electrophoresis in microchannels is relevant to many applications. It has long been accepted that particles move parallel to the applied electric field in a straight uniform microchannel. This paper presents the first experimental demonstration of lateral particle migration in electrophoresis through a rectangular microchannel. This wall-induced dielectrophoresis-resembled motion is driven by the electrical force arising from the non-uniform electric field around the particle. It decays rapidly when the particle is away from the channel wall, and vanishes in the center of the channel. The observed result is a focused particle stream flowing along the channel centerline. The measured widths of the particle stream at various electric fields agree reasonably with the predictions of an approximate analytical model.

© 2010 Elsevier Inc. All rights reserved.

1. Introduction

The fundamental study of particle electrophoresis in confined microchannels is relevant to many applications such as gel electrophoresis [1] and various microfluidic particle-handling devices [2]. Owing to the spontaneous charging of most solid surfaces when brought into contact with polar liquids like water [3], the observed particle motion in electrophoresis through microchannels is typically a combination, but not just a simple addition, of particle electrophoresis and liquid electroosmosis [4].

There have appeared a number of theoretical and experimental papers investigating the wall effects on particle electrophoretic motion in microchannels. These studies can be coarsely divided into two groups: one is on particle electrophoresis in a straight uniform microchannel of, for example, slit, cylindrical, or rectangular shape where the electric field distribution is uniform [5–28], and the other is on particle electrophoresis in either a non-uniform [29–36] or a nonstraight [37–41] microchannel where electric field gradients are present. In the latter case, particle dielectrophoresis is usually induced, which has been exploited to focus [35,39,40], trap/concentrate [42–45], and separate particles [45–49]. Such cross-stream motion has, however, been deemed to be absent in particle electrophoresis through a straight uniform microchannel.

Recently, Yariv [50] demonstrated through a theoretical analysis that a particle drifts away from a wall under an electric field acting parallel to the wall. This lateral migration, which is superimposed to the familiar particle electrophoretic motion parallel to the wall, is induced by a nonzero electrical force resulting from the non-uniform electric field around the particle. A similar force was also considered by Young and Li [51] in an earlier theoretical study to determine the equilibrium height of a colloidal particle during electrophoretic motion above a planar wall. It was found that the gap distance between the particle and the planar wall could be on the order of a few micrometers.

This paper is aimed to provide the first experimental demonstration of the wall-induced lateral migration in particle electrophoresis through a straight uniform microchannel of rectangular shape. An approximate analytical model is also developed to predict and compare with the experimental observations.

2. Experiment

2.1. Microchannel fabrication

The microchannel was fabricated with polydimethylsiloxane (PDMS) using the standard soft lithography method [52]. The channel geometry was designed in AutoCAD, and printed onto a thin transparent film that later served as a negative photomask. Photoresist (SU-8 25, MicroChem Corp., Newton, MA) was dispensed onto a glass slide by spin-coating (WS-400E-NPP-Lite, Laurell Technologies, North Wales, PA), which yielded a uniform thickness of 25 μm. The slide was then subjected to a two-step soft bake at 65 and 95 °C, respectively, to evaporate the solvent and densify

* Corresponding author. Fax: +1 864 656 7299.
E-mail address: xcxuan@clemson.edu (X. Xuan).

0021-9797/$ - see front matter © 2010 Elsevier Inc. All rights reserved.
doi:10.1016/j.jcis.2010.03.039

Author's personal copy

the resist film. Following that, the resist was covered by the photomask for near-UV light exposure (ABM Inc., San Jose, CA). After a two-step postexposure bake at 65 and 95 °C, the photoresist was developed in SU-8 developer forming the positive mold of the designed microchannel for PDMS casting.

The channel mold was put into a petri dish and covered with liquid PDMS (Dow Corning Corp., Midland, USA). After being degassed in an isotemp vacuum oven (13-262-280A, Fisher Scientific, Fair Lawn, NJ) for 30 min, the liquid PDMS was cured in a gravity convection oven (13-246-506GA, Fisher Scientific) at 70 °C for 2 h. Once cured, the PDMS with the channel portion was cut out and placed onto a clean glass slide with the channel side facing down. Two 5-mm-diameter through holes were then punched in the predesigned regions for reservoirs. Subsequently, the channel side of the PDMS slab was plasma-treated (PDC-32G, Harrick Scientific, Ossining, NY) along with another clean glass slide for 1 min. Immediately following that, the two treated surfaces were bonded to form the microchannel.

Fig. 1 shows a picture of the fabricated microchannel in this work. It consists of an 8-mm-long uniform section in the middle and a 1-mm-long diffuser at each end. So the overall length of this straight channel is 10 mm as indicated in the figure. The entire channel owns a rectangular cross section with a fixed depth of 25 μm. The channel width in the uniform section is 50 μm.

2.2. Particle manipulation

Spherical polystyrene particles (Sigma–Aldrich USA) of two different sizes, 5 and 10 μm in diameter, were used in our experiments. The original particle solution was diluted with 1 mM phosphate buffer to a final concentration of about 10^7 particles per milliliter, for both sizes of particles. Tween 20 (Fisher Scientific) was added at a volume ratio of 0.5% to the particle solutions for reducing the particle adhesions to channel walls.

Electric field was generated by applying a DC voltage drop between the two electrodes that were in contact with the solution in the two reservoirs. The DC voltages of various magnitudes were supplied by a DC power supply (Glassman High Voltage Inc., High Bridge, NJ). Pressure-driven flow was eliminated by carefully balancing the liquid heights in the two reservoirs prior to each measurement. Particle motion was visualized and recorded using an inverted microscope (Nikon Eclipse TE2000U, Nikon Instruments, Lewisville, TX) equipped with a CCD camera (Nikon DS-Qi1Mc). The obtained videos and images were then processed using the Nikon imaging software (NIS-Elements AR 2.30).

3. Theory

3.1. Mechanism of lateral particle migration

Consider a nonconducting particle of radius a moving electrophoretically through a rectangular microchannel of half width w_c at a velocity of $\mathbf{U}_{EK}$ (a combination of particle electrophoresis and fluid electroosmosis [3,4]). The separation distance between the particle and the closer sidewall is assumed to be γ, which in principle may vary from 0 (i.e., in touch with the sidewall) to (w_c–a) (i.e., along the channel centerline). Fig. 2 shows the electric field lines and contours (the darker the larger) around this particle in the horizontal plane of the channel. The computation was performed in COMSOL (Burlington, MA), which will be explained in Section 3.2. The finite-size particle causes distortions to the electric field lines and creates electric field gradients around it. In the channel length direction (i.e., x direction in Fig. 2), the electric field distribution is symmetric about the particle, leading to zero electrical force in the particle moving direction.

In the channel width direction (i.e., y direction in Fig. 2), however, the particle experiences a net electrical force due to the asymmetric electric field around its two poles. Note that in the traditional analysis of particle electrophoresis in both bounded and unbounded flows, the electrical force on the neutral system of particle and electrical double-layer is assumed zero. This wall-induced repulsive force [30,50,51], $\mathbf{F}_w$, causes a lateral particle migration toward the channel center, denoted as $\mathbf{U}_w$ in Fig. 2. Such a lateral migration also takes place in the channel depth direction. It is therefore anticipated that neutrally buoyant particles in electrophoresis should be ultimately traveling along the centerline of a sufficiently long microchannel. In this work the polystyrene particles are slightly heavier than the suspending fluid, and thus should migrate vertically to an equilibrium position below the channel axis.

3.2. Simulation of particle trajectory

In simulating the particle trajectory, the following assumptions have been made: (1) particles and channel walls are nonconducting; (2) fluid properties remain uniform throughout the channel; (3) Reynolds number is very small, and so inertia is negligible; (4) the rotation of a particle does not affect its translation; and (5) particle–particle interaction is negligible.

The instantaneous position of the center of a particle, $\mathbf{r}_p$, is obtained by integrating the particle velocity, $\mathbf{u}_p$, with respect to time, t,

$$\mathbf{r}_p = \mathbf{r}_0 + \int_0^t \mathbf{u}_p(t')\,dt', \tag{1}$$

where $\mathbf{r}_0$ is the initial position of the particle center, and was assumed to be $(0, a)$ in the calculation. In the x direction, the electrokinetic particle velocity is known to vary with the particle–wall separation distance [4]. However, this variation is generally very small unless the particle is nearly in contact with the wall or closely fitting the channel [7,13,53,54]. The former condition is not fulfilled in this work as particles are unable to approach the channel sidewall in close proximity due to the wall-induced repulsive force, $\mathbf{F}_w$; see Fig. 2. The condition of closely fitting particles is not applicable in this work, either, as the sizes of the two particles (5 and 10 μm in diameter) are both much smaller than the width of the

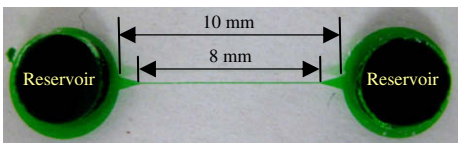

Fig. 1. Picture and dimensions of the rectangular microchannel used in the experiment.

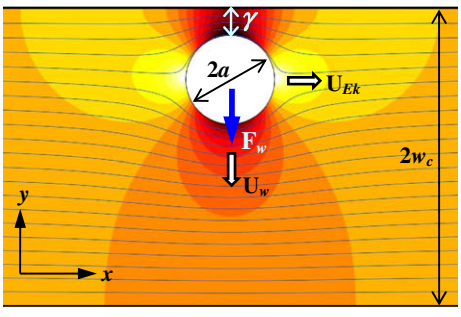

Fig. 2. Velocity analysis (in the horizontal plane) of a particle in electrophoretic motion through a rectangular microchannel. The background shows the electric field contours (the darker the larger) and lines.

Author's personal copy

microchannel (50 μm). Therefore, the streamwise electrokinetic velocity, $\mathbf{U}_{EK}$, is assumed insensitive to the particle–wall separation distance in this approximate analytical model, which is also confirmed by the present and previous experiments [16]. Thus, Eq. (1) is reduced to

$$x_p = \mu_{EK} E t, \tag{2}$$

where μ_{EK} is the electrokinetic particle mobility, and E is externally applied electric field in the uniform channel section.

In the y direction, Eq. (1) is rewritten as

$$y_p = a + \gamma = a + \int_0^t U_w(t')\,dt', \tag{3}$$

where the lateral particle migration velocity, U_w, can be obtained by balancing the wall-induced repulsive force, $\mathbf{F}_w$, with the Stokes drag force. The magnitude of this electrical force, F_w, can be determined by integrating the Maxwell stress tensor over the particle surface. Here, the analytical expression provided by Yariv [50] is adapted to account for the net force arising from the two sidewalls,

$$F_w = \frac{3\pi}{16}\left[\left(\frac{a}{\gamma + a}\right)^4 - \left(\frac{a}{2w_v - \gamma - a}\right)^4\right]\varepsilon_f a^2 E^2, \tag{4}$$

where ε_f is the fluid permittivity. Thus, the lateral particle migration velocity can be obtained as

$$U_w = \frac{\varepsilon_f}{32\mu_f} a E^2 \left[\left(\frac{a}{\gamma + a}\right)^4 - \left(\frac{a}{2w_v - \gamma - a}\right)^4\right], \tag{5}$$

where μ_f is the dynamic viscosity of the suspending fluid. In deriving Eq. (5), the Stokes drag coefficient has been assumed constant for simplicity, which is admitted to break down when particles move in close proximity to a channel wall [55]. Apparently U_w increases with the particle size and the applied electric field, but decays rapidly with the increase of the particle–wall separation distance, γ. Additionally it is important to note that the dielectrophoresis-resembled force, $\mathbf{F}_w$, is different from the electrical double-layer interaction between the particle and the wall. The latter force occurs only when γ is in the order of nanometers [56].

The simulation of particle trajectory was carried out in MATLAB using Eqs. (2) and (3). The obtained lateral particle position, y_p, at a given location, x_p, of the channel length was then used to calculate the half width, w_p, of the particle stream,

$$w_p = w_c - y_p + a = w_c - \gamma. \tag{6}$$

Note that w_p is assumed to be equal to the half channel width, w_c, at $t = 0$. The predicted particle stream width, $2w_p$, is compared with the width of the experimentally recorded particle streaks.

The following parameters were needed in the simulation: (1) the electric field in the uniform section of the microchannel in the absence of particles was computed from a 2D model in COMSOL, which considered the full size of the channel and reservoirs. For example, a 300 V DC voltage drop imposed across the channel length produces an electric field of 34.9 kV/m in the uniform section, which is stated as the nominal electric field of 30 kV/m hereafter for simplicity; (2) the electrokinetic particle mobility, μ_{EK}, was determined by dividing the measured particle velocity in the uniform channel section at a nominal electric field of 30 kV/m by the real electric field of 34.9 kV/m. This relative small field ensures that Joule heating effects were negligible in the 50-μm-wide channel during the measurement [57]. The obtained μ_{EK} is 2.7×10^{-8} m^2/(V s) for both 5- and 10-μm particles used in the experiment; (3) the properties of the suspending fluid were assumed to be identical to those of water at 20 °C, which include the dynamic viscosity, $\mu_f = 0.9 \times 10^{-3}$ kg/(m s) and permittivity, $\varepsilon_f = 6.9 \times 10^{-10}$ C/(V m).

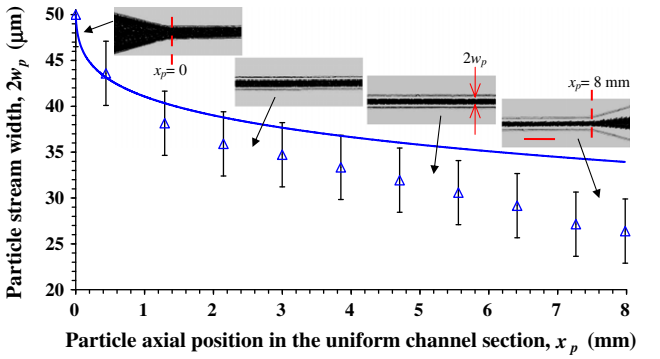

Fig. 3. Variation of the stream width, $2w_p$ (see the labeled dimension in the inset), of 5-μm particles with the axial traveling distance in the uniform section of the microchannel under a nominal electric field of 30 kV/m. Symbols (with error bars) represent the experimental data while the solid line illustrates the numerically predicted results. The four insets show the superimposed particle images at the entrance, exit, and two intermediate regions of the uniform channel section, respectively. The scale bar represents 100 μm.

4. Results and discussion

4.1. Effect of axial traveling distance

Fig. 3 shows how the stream width, $2w_p$, of 5-μm particles varies with the axial traveling distance, x_p, during electrophoresis in the uniform section of the straight microchannel. The experimental data (symbols) were obtained by measuring the width of the particle stream in the superimposed images (see the insets and the labeled dimension $2w_p$). Considering the possible error of ±1 pixels in reading the edges of the particle stream, an error bar of ±3.5 μm has been added to the experimental data. Due to the wall-induced lateral migration, particles are observed to migrate toward the channel center, leading to a gradually decreased stream width along the channel length. At the entrance of the uniform section (i.e., $x_p = 0$ in Fig. 3; see also the highlight in the inset), the particles appear uniformly distributed forming a stream of channel wide (i.e., 50 μm). The width of this stream first quickly drops to less than 40 μm within the first 1-mm-long channel, and then decreases slowly to about 26 μm in the next 7-mm-long section. These varied decreasing trends arise from the fourth-power dependence of the electrical force, i.e., F_w in Eq. (4), on the particle–wall separation distance, which are correctly predicted by the analytical model (solid line) as seen in Fig. 3. However, the model underpredicts the lateral particle migration due to the approximate treatment of F_w.

4.2. Effect of electric field

Fig. 4 shows the images (left, snapshot; right, superimposed) of 5-μm particles recorded at the exit region of the uniform channel section under different electric fields: (b) 10 kV/m, (c) 30 kV/m, and (d) 50 kV/m. The particle images at the entrance region (Fig. 4a) are also included for a clear comparison, which remain nearly the same when the electric field is varied. Obviously increasing the field magnitude enhances the lateral particle migration. This is as expected because the width of the particle stream is determined by the ratio of the distance the particle moves laterally to the distance the particle moves longitudinally, which can be expressed as the ratio of the particle's lateral migration velocity to the streamwise electrokinetic velocity,

$$\frac{U_w}{U_{EK}} = \frac{\varepsilon_f\left[\left(\frac{a}{a+\gamma}\right)^4 - \left(\frac{a}{2w_c - a - \gamma}\right)^4\right]}{32\mu_f}\frac{aE}{\mu_{EK}}. \tag{7}$$

Author's personal copy

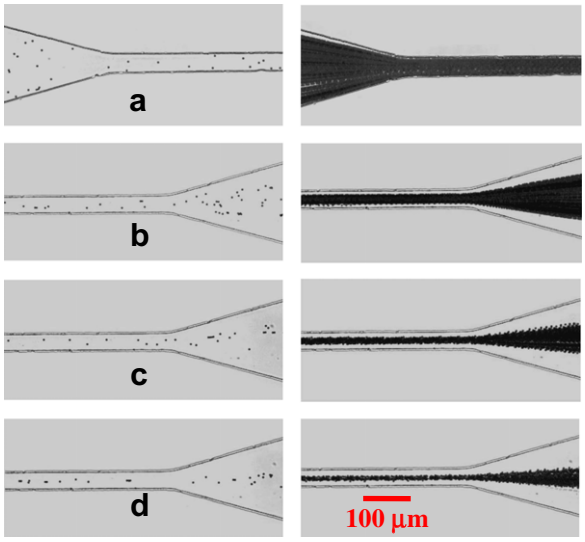

Fig. 4. Snapshot (left column) and superimposed (right column) images of 5-μm particles moving at the entrance (a) and exit (b–d) regions of the uniform section of the straight microchannel. The nominal electric fields in (b), (c), and (d) are 10, 30, and 50 kV/m, respectively.

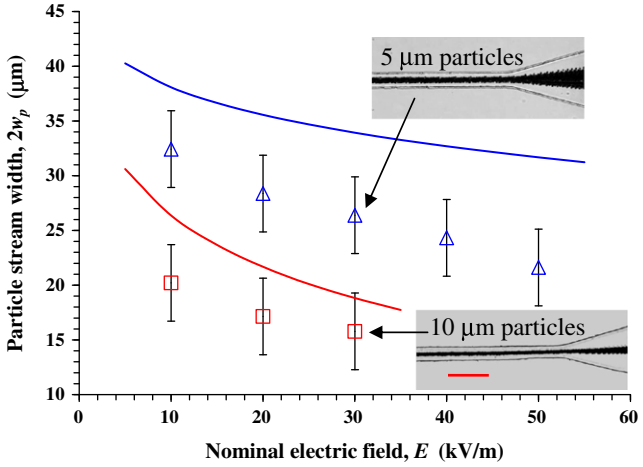

Fig. 5. Electric field and particle size effects on the particle stream width at the exit of the uniform section of the microchannel. Symbols (with error bars) represent the experimental data while solid lines are numerically predicted results. The two insets display the superimposed images of 5- and 10-μm particles under the nominal electric field of 30 kV/m. The scale bar represents 100 μm.

Since the electrokinetic particle mobility, μ_{EK}, is in general not dependent on the applied electric field, the above velocity ratio increases linearly with electric field, yielding a thinner particle stream along the channel axis as demonstrated in Fig. 4.

The experimentally measured stream widths of 5-μm particles (triangular symbols with error bars) at the exit of the uniform channel section are compared with the numerically obtained values (the longer solid line) in Fig. 5 for a range of electric fields. While it predicts correctly the decreasing trend of the particle stream width with respect to electric field, the model appears to underpredict the lateral particle migration, especially significant at large electric fields. This discrepancy is believed to be the consequence of the approximation of the wall-induced electrical force and the neglect of particle–particle interactions in our model as these two forces both increase with increasing electric field.

4.3. Effect of particle size

Fig. 5 also illustrates the experimentally (square symbols with error bars) and numerically (the shorter solid line) obtained stream widths of 10-μm particles at the exit of the uniform channel section at various electric fields. Compared to that of 5-μm particles, the lateral migration of 10-μm particles is much more apparent (see the two inset images in Fig. 5). This observation correlates well with the prediction of Eq. (7). As the measured electrokinetic mobilities of the two particles are roughly identical, the velocity ratio, U_w/U_{EK}, of 10-μm particles is certainly larger than that of 5-μm particles. At the electric field of 10 kV/m, the lateral migration can already focus 10-μm particles from a stream of channel wide (i.e., 50 μm) at the entrance to a stream of 21 μm wide at the exit of the uniform section. When the electric field increases to 30 kV/m, 10-μm particles basically can only migrate in a single file because the measured particle stream width is decreased to about 15 μm. This focusing phenomenon in particle electrophoresis, which will become more pronounced in a longer microchannel as evidenced in Fig. 3, might be potentially used in microfluidic flow cytometry [58–60]. In addition, similar to what was discussed earlier for 5-μm particles, the numerical model also underpredicts the lateral migration of 10-μm particles though to a smaller extent.

5. Conclusions

Lateral migration in particle electrophoresis through a straight uniform microchannel has been experimentally demonstrated for the first time. It results from the electrical force induced by the non-uniform electric field around the particle. This wall-induced cross-stream motion has been observed to gradually focus 5- and 10-μm-diameter polystyrene particles to a stream flowing in the center region of a 50-μm-wide rectangular microchannel. The width of the particle stream at the channel exit is found to decrease with the increase in either particle size or electric field. The measured values of the stream width are in reasonable agreement with the predictions of an approximate analytical model. It is envisioned that the lateral particle migration in microchannel electrophoresis may be utilized to implement a three-dimensional focusing of cells for the application of microflow cytometry.

Acknowledgments

This work was supported by NSF under Grant CBET-0853873 with Marc S. Ingber as the grant monitor (XX), and in part, by Ministry of Education, Science, and Technology of Korea World Class University (WCU) Program (SQ).

References

[1] J. Viovy, Rev. Mod. Phys. 7 (2000) 813–872.
[2] Y. Kang, D. Li, Microfluid. Nanofluid. 6 (2009) 431–460.
[3] R.J. Hunter, Zeta Potential in Colloid Science, Principles and Applications, Academic Press, New York, 1981.
[4] J.L. Anderson, Annu. Rev. Fluid Mech. 21 (1989) 61–99.
[5] H.J. Keh, J.L. Anderson, J. Fluid. Mech. 153 (1985) 417–439.
[6] H.J. Keh, L.C. Lien, J. Fluid Mech. 224 (1991) 305–333.
[7] H.J. Keh, J.Y. Chiou, AIChE J. 42 (1996) 1397–1406.
[8] A.A. Shugai, S.L. Carnie, J. Colloid Interface Sci. 213 (1999) 298–315.
[9] C. Ye, D. Sinton, D. Erickson, D. Li, Langmuir 18 (2002) 9095–9101.
[10] E. Yariv, H. Brenner, SIAM J. Appl. Math. 64 (2003) 423–441.
[11] J.P. Hsu, M.H. Ku, C.Y. Kao, J. Colloid Interface Sci. 276 (2004) 248–254.
[12] H. Liu, H.H. Bau, H.H. Hu, Langmuir 20 (2004) 2628–2639.
[13] C. Ye, X. Xuan, D. Li, Microfluid. Nanofluid. 1 (2005) 234–241.
[14] X. Xuan, C. Ye, D. Li, J. Colloid Interface Sci. 289 (2005) 286–290.
[15] S.M. Davison, K.V. Sharp, J. Colloid Interface Sci. 303 (2006) 288–297.
[16] X. Xuan, R. Raghibizadeh, D. Li, J. Colloid Interface Sci. 296 (2006) 743–748.
[17] J.P. Hsu, C.C. Kuo, J. Phys. Chem. B 110 (2006) 17607–17615.
[18] S.M. Davison, K.V. Sharp, Nanoscale Microscale Thermophys. Eng. 11 (2007) 71–83.

Author's personal copy

[19] H. Liu, S. Qian, H.H. Bau, Biophys. J. 92 (2007) 1164–1177.
[20] T.H. Hsieh, H.J. Keh, J. Colloid Interface Sci. 315 (2007) 343–354.
[21] H.N. Unni, H.J. Keh, C. Yang, Electrophoresis 28 (2007) 658–664.
[22] J.P. Hsu, Z.S. Chen, Langmuir 23 (2007) 6198–6204.
[23] S. Tseng, C.H. Cho, Z.S. Chen, J.P. Hsu, Langmuir 24 (2008) 2929–2937.
[24] S.Z. Qian, S.W. Joo, Langmuir 24 (2008) 4778–4784.
[25] S.Z. Qian, S.W. Joo, W.S. Hou, X.X. Zhao, Langmuir 24 (2008) 5332–5340.
[26] L.J. Wang, H.J. Keh, J. Phys. Chem. C 113 (2009) 12790–12798.
[27] Y. Ai, A. Beskok, D.T. Gauthier, S.W. Joo, S. Qian, Biomicrofluidics 3 (2009) 044110.
[28] D. Li, Y. Daghighi, J. Colloid Interface Sci. 342 (2010) 638–642.
[29] X. Xuan, B. Xu, D. Li, Anal. Chem. 77 (2005) 4323–4328.
[30] K.H. Kang, X. Xuan, Y. Kang, D. Li, J. Appl. Phys. 99 (2006) 064702.
[31] S.Z. Qian, A.H. Wang, J.K. Afonien, J. Colloid Interface Sci. 303 (2006) 579–592.
[32] E. Yariv, K.D. Dorfman, Phys. Fluid. 19 (2007) 037101.
[33] K.D. Dorfman, Phys. Fluid. 20 (2008) 037102.
[34] Y. Ai, S.W. Joo, Y. Jiang, X. Xuan, S. Qian, Electrophoresis 30 (2009) 2499–2506.
[35] J. Zhu, X. Xuan, Electrophoresis 30 (2009) 2668–2675.
[36] Y. Ai, S. Qian, S. Liu, S.W. Joo, Biomicrofluidics 4 (2010) 013201.
[37] C. Ye, D. Li, J. Colloid Interface Sci. 272 (2004) 480–488.
[38] S.M. Davison, K.V. Sharp, Microfluid. Nanofluid. 4 (2008) 409–418.
[39] J. Zhu, T.R. Tzeng, G. Hu, X. Xuan, Microfluid. Nanofluid. 7 (2009) 751–756.
[40] J. Zhu, X. Xuan, J. Colloid Interface Sci. 340 (2009) 285–290.
[41] Y. Ai, S. Park, J. Zhu, X. Xuan, A. Beskok, S. Qian, Langmuir 26 (2010) 2937–2944.
[42] B.H. Lapizco-Encinas, B.A. Simmons, E.B. Cummings, Y. Fintschenko, Anal. Chem. 76 (2004) 1571–1579.
[43] B.H. Lapizco-Encinas, B.A. Simmons, E.B. Cummings, Y. Fintschenko, Electrophoresis 25 (2004) 1695–1704.
[44] M.D. Pysher, M.A. Hayes, Anal. Chem. 79 (2007) 4552–4557.
[45] B.G. Hawkins, A.E. Smith, Y.A. Syed, B.J. Kirby, Anal. Chem. 79 (2007) 7291–7300.
[46] K.H. Kang, Y. Kang, X. Xuan, D. Li, Electrophoresis 27 (2006) 694–702.
[47] Y. Kang, D. Li, S.A. Kalams, J.E. Eid, Biomed. Microdev. 10 (2008) 243–249.
[48] N. Lewpiriyawong, C. Yang, Y.C. Lam, Biomicrofluidics 2 (2008) 034105.
[49] J. Zhu, T.R. Tzeng, X. Xuan, Electrophoresis 31, in press. doi:10.1002/elps.200900736.
[50] E. Yariv, Phys. Fluid. 18 (2006) 031702.
[51] E. Young, D. Li, Langmuir 21 (2005) 12037–12046.
[52] D.C. Duffy, J.C. McDonald, O.J.A. Schueller, G.M. Whitesides, Anal. Chem. 70 (1998) 4974–4984.
[53] H.J. Keh, S.B. Chen, J. Fluid. Mech. 194 (1988) 377–390.
[54] E. Yariv, H. Brenner, Phys. Fluid. 14 (2002) 3354–3357.
[55] J. Happel, H. Brenner, Low Reynolds Number Hydrodynamics, Noordhoff, Leyden, Netherlands, 1973.
[56] J.N. Israelachvili, Intermolecular and Surface Forces, second ed., Academic Press, San Diego, 1991.
[57] X. Xuan, Electrophoresis 29 (2008) 33–43.
[58] T.D. Chung, H.C. Kim, Electrophoresis 28 (2007) 4511–4520.
[59] D.A. Ateya, J.S. Erickson Jr, P.B. Howell, L.R. Hilliard, J.P. Golden, F.S. Ligler, Anal. Bioanal. Chem. 391 (2008) 1485–1498.
[60] J. Godin, C. Chen, S.H. Cho, W. Qiao, F. Tsai, Y. Lo, J. Biophotonics 1 (2008) 355–376.